



Seasonal behavior and techno economical analysis of a multi-stage solar still coupled with a point-focus Fresnel lens

Obaid Younas^a, Fawzi Banat^{a,*}, Didarul Islam^b

^aDepartment of Chemical Engineering, The Petroleum Institute, Sas Al Nakhl, P.O. Box 2533 Abu Dhabi, United Arab Emirates, Tel. +97126048742; email: obaidy@adco.ae (O. Younas), Tel. +97126075099; email: fbanat@pi.ac.ae (F. Banat)

^bDepartment of Mechanical Engineering, The Petroleum Institute, Sas Al Nakhl, P.O. Box 2533 Abu Dhabi, United Arab Emirates, Tel. +97126075230; email: dislam@pi.ac.ae

Received 16 July 2014; Accepted 17 December 2014

ABSTRACT

A multi-stage solar still (MSS) was coupled with a point-focus Fresnel lens for the desalination of saline water. The system was tested in field conditions at The Petroleum Institute, Abu Dhabi. A transient mathematical model was developed for the system. Modeling results show a deviation of about 5% in daily yield of MSS when compared with the experimental results. Based on the average hourly direct beam radiation data for a complete year, the model was used for the determination of seasonal behavior of a MSS. The systems' seasonal behavior shows that maximum productivity of 10 kg/m² d (based on evaporation area) was achieved in the months of May and June, while the productivity was the lowest at 4.8 kg/m² d in the month of December. Different design parameters were tested to enhance the daily output of the current system. The parametric optimization study suggests that a maximum daily productivity of about 5 kg/m² d or 11.4 kg/m² d (based on solar collector area) can be achieved through the system. Cost optimization was performed for the determination of parameters that will result in maximum MSS daily output at lowest expense. The cost optimized parameters were determined for five stages, with 1.0 m² evaporation area for each stage, 10 cm stage spacing and a Fresnel lens of area 2.2 m². The unit production cost competes well with earlier developed solar desalination systems and the payback period is about one year.

Keywords: Multi stage solar still; Fresnel lens; Renewable energy; Desalination

1. Introduction

Simple solar stills appear to be a good option for remote areas which suffer from shortage of infrastructure. However, high production cost, low efficiency, low productivity, and a large footprint are the main hurdles for wide adoption of these small plants. One

of the possible solutions is the use of multi-stage active solar stills coupled with solar collection system. Nowadays, research activities are focusing to increase the still productivity, reliability, and reduce cost of solar stills coupled with solar collection systems. Such investigations involve new designs of solar distillation systems that improve output through the increase of water temperature in the still. This can be achieved by heat recovery in multi-stage solar stills (MSSs).

*Corresponding author.

To study the effect of various parameters affecting the performance of MSS, different researchers performed numerical calculations based on software available on computer modeling. Most of these reported models use fix value of irradiation and steady state operation. Tiwari et al. [1] conducted simple analytical study of the multi-effect wick type solar still incorporating the effect of various parameters. These parameters included still length, water flow velocity, inclination of absorber, and the optimum number of condensing surface area. Also, numerical calculations were carried out for the determination of hourly yield from still. A computer-based simulation model for studying the transient performance of a multi-stage stacked tray solar still was developed by Adhikari and Kumar [2]. The model was validated against indoor experiments on a three-stage solar still having electric heater as the heating source. Numerical calculations were made to evaluate the performance of the system heated by a solar collector. Effects of number of stages and ratio of collector area to the bottom tray area on the distillate output were also studied. A double effect active solar distillation unit coupled with compound parabolic concentrator (CPC) has been presented by Prasad and Tiwari [3]. Incorporating the effects of climatic as well as design parameters, an analytical expression for hourly yield contributed by each effect was derived. For an evaporation area of 2 m² the distillate output ranged between 10.8 and 14.6 kg. Ahmed et al. [4] performed experiments and developed a mathematical model for a third-stage MSS under vacuum. Maximum distillate flux of 14.2 kg/m² d with a vacuum pressure of 0.5 bar was reported. Shatat and Mahkamov [5] coupled evacuated tube solar collector (2.2 m²) with four-effect MSS. Further, a mathematical model was developed for transient simulation of condensation and evaporation. The indoor experiments conducted showed a daily output of 9 kg and a flux of 11 kg/m² d were reported on the basis of simulations performed.

Most of the above mentioned models either used correlations for predicting convective heat transfer in the still or they used fixed values of “*c*” and “*n*” (for given G_r range), which appear in Nusselt number expression. In an attempt to increase the accuracy of the developed model, Kumar and Tiwari [6] proposed modified values of “*c*” and “*n*” for the estimation of heat transfer coefficients in distillation chamber. These modified values of “*c*” and “*n*” were determined from experimental data through simple regression analysis. The maximum reported deviation in hourly yield was only 12%. Models developed using modified “*c*” and “*n*” values for a double slope solar still and a simple solar still [7] showed distillate output deviation of 16.3

and 17%, respectively. Khaoula et al. [8] used the modified values of “*c*” and “*n*” for numerical calculations on simple solar still with heat pump. They reported a deviation 5–21% for the developed models.

The current study involves the exploration of a new active solar thermal desalination system. A small multi-effect solar still was designed, fabricated, and coupled with a point focus Fresnel lens. The system was tested in field conditions at The Petroleum Institute, Abu Dhabi, UAE and a transient mathematical model was developed [2,5]. This model served to be a guide for parametric and economical study.

2. Theory

2.1. System description

2.1.1. Multi-effect solar still (MSS)

A three-stage MSS unit for the desalination of saline water was built and tested at The Petroleum Institute, Abu Dhabi. Galvanized iron (GI) was selected as material of construction. The basic schematic of the developed system is presented in Fig. 1. It was designed into two parts, the base of the still as first part, was constructed using 3 mm thick GI sheet to accommodate corrosion allowance. Because of higher temperature in first stage, the chances of corrosion were higher in presence of saline water. An inclined 2 mm copper plate with 50° angle of inclination was chosen in front side of the still to receive the sun light. Due to top inclination, the length of the still base varied from 600 to 493 mm from bottom to top with height of 127 mm for the still base. The next part was fabricated with 2 mm GI sheets. Mild steel hollow square columns with 37.5 × 37.5 mm² area and 833 mm height were used to support the structure. These support columns were slide and welded into the base still to form the backside of still. At a distance of 333 mm from the bottom of back side and 200 mm from the bottom of front side, a GI sheet was welded at 15° inclination to form the condensing cover for the first stage. Another GI sheet was welded at 250 mm above the first stage to form the second stage condensing surface. Each stage was provided with openings for saline water inlet, drain for brine, level indicator, and thermocouple fittings. Distillate collection troughs were welded beneath the condensing cover on front side. For the condensing surface of last stage a clear glass sheet with area of 510 × 500 mm was used.

The still had a height of 833 mm and width of 500 mm. For the 1st stage the average length was 550 mm while the rest of the stages had uniform lengths of 493 mm.

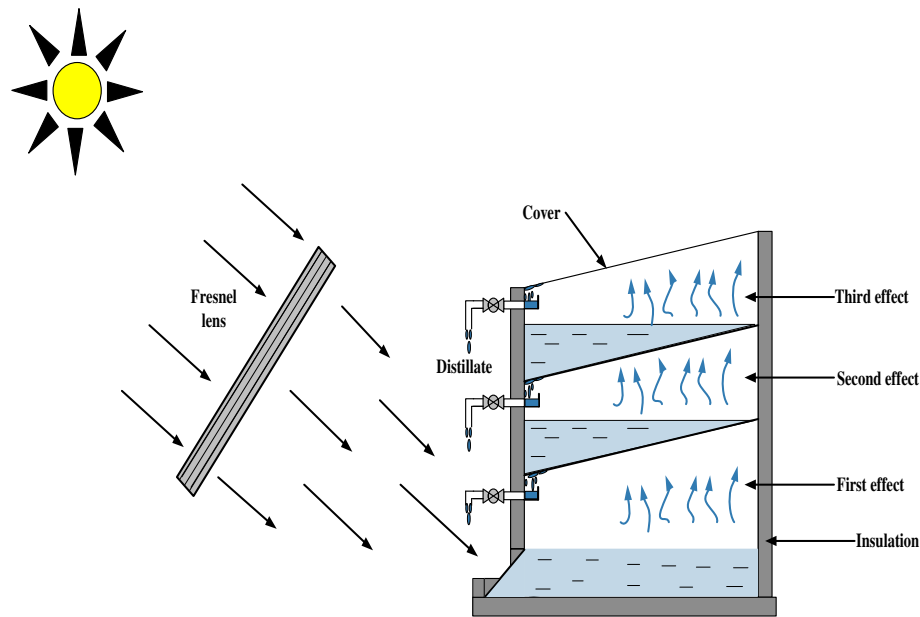


Fig. 1. Schematics of solar thermal desalination.

2.1.2. Fresnel lens

The Fresnel lens was invented by Augustin Jean Fresnel in 1822. The conventional spherical lenses produce a focus image that suffers longitudinal spherical aberration; non-sharp focus. The problem of spherical aberration can be avoided using aspheric lenses. The surface contour of aspheric lens is modified in such a way so as to bring rays passing through all the points on the lens to focus at the same position on the optical axis. A Fresnel lens is an aspheric lens engineered to the form of a thin sheet. The solar concentrating Fresnel lens (CF1200-B3) used in these experiments was made of Plexiglas/Polymethylmethacrylate, manufactured by NTKJ Japan. The lens has a focal length of 1200 mm and effective area of 1.37 m². It has a transmission efficiency of 0.85 as per manufacturer's specified information. The advantages of using Fresnel lenses are (i) Plexiglas which is cheaper and durable, (ii) the spot temperatures produced are as good as produced by PDR, (iii) it does not require heavy maintenance, (iv) reported operating life is more than 30 years, and (v) the cost of Fresnel lens ranges \$140–160/m².

2.1.3. Mechanical tracking system

The mechanical tracking system served not only for tracking sun but also holds the weight of MSS unit and Fresnel lens. The tracking system consisted of a lens frame connected to base frame through support

and sliding rods. The lens frame could be rotated about lens' focal point in order to cover the zenith angle; the angle between sun and vertical, zero at sun rise and sun set, and almost 90° at noon. This lens frame is connected to two support rods which can slide along two other rods; hence, enabling the lens for the zenith angle tracking. All of these support rods are attached to a base frame on which solar MSS unit is placed in such a position that it can receive concentrated sun light on inclined front plate of still base. Four wheels are attached to the base plate so that it can be moved/rotated to cover azimuth angle; the angle between south and the direction that the solar collector is facing.

2.1.4. Instrumentation and measurements

For the measurement of temperatures, beam solar irradiance, amount of distillate, and wind velocity several instruments were used. These include pyrheliometer (to measure the direct beam solar irradiance), thermocouples, measuring cylinders, and anemometer. The temperature of water was measured using class-2 type-k thermocouples (accuracy $\pm 1.5^\circ\text{C}$) with stainless steel sheath suitable for high pressure applications. These thermocouples were fitted using compression fittings to the drain point of each stage. For the measurement of condensing surface temperature and front plate temperatures, thermocouples were installed on these surfaces. The thermocouples were of the

class-1 k-type self-adhesive (accuracy $\pm 0.5^\circ\text{C}$) variety. These thermocouples are suitable for surface temperature measurement. The ambient temperature and wind speed were measured with Xplorer2 anemometer, having in-built thermometer for ambient temperature measurement. The temperature accuracy of Xplorer2 was $\pm 0.3^\circ\text{C}$ and wind speed accuracy was $\pm 3\%$.

Simple level indicators made of transparent rubber house were installed near drain point of every stage. Drain valves were provided for the drainage of each stage. Graduated measuring cylinders were used for the collection and measurement of desalinated water. The whole MSS was insulated to avoid heat loss.

2.1.5. Experimental procedure

To hold desired quantities of water in each stage, basin of each stage was calibrated for the water mass in terms of water column height. The first stage contained 15 kg of saline water (56 mm water column height) and the rest of the stages had 14.2 kg of saline water (115 mm). Initial temperature of water in the basin, condensing surface temperatures of each stage, front plate temperature, and ambient temperature were recorded.

The experiment was started by adjusting lens orientation so that the concentrated spot was focused on first stage of the front plate. The spot was kept focused on a specific area of front plate with the help of tracking mechanism. The tracker needed adjustment after every 5–10 min. After 1 h, the increase in temperature for waterbed, condensing surfaces, and ambient temperature were recorded. The condensate outlet valves were opened to collect any distillate in measuring cylinders. The still was heated for a continuous period of 5–7 h.

The condensed water vapors crept along the cover sheet and moved into the collection trough. The heated water in upper stage produced vapors which in turns heats water in the next stage. The phenomena of subsequent evaporation and condensation remained same throughout the MSS.

2.2. Model assumptions

The following assumptions were made while developing the model:

- The temperature-dependent physical properties of fresh water and saline water are the same.
- The product water, leaving a stage is at a temperature equal to the condensing surface temperature of that particular stage.

- The average temperature of day and weighted average temperature of night are implemented separately.
- The heat losses from still walls, base, front plate, and from the top glass cover occur due to convection and radiation.
- All of the evaporated water in a stage becomes distillate product of that stage.
- The heat transfer inside MSS is governed by convection, evaporation, and radiation.
- The model simulates the MSS behavior for 24 h run, which include both the heating period and cooling period of still.

2.3. Model development

The developed model is a transient mathematical model which utilizes the empirical equations derived from the experimental results. Since, the study was conducted outdoor; incorporating uncontrolled variables was a challenge. The model uses ambient temperatures of day and night separately along with wind speed for improving the accuracy of results. It uses modified values of “*c*” and “*n*” for the prediction of heat transfer coefficients for the improvement of predictions. The developed mathematical model is based on a set of ordinary differential equations derived by applying heat and mass balances on individual stages. The set of equations were then solved with the aid of a program written in MATLAB. The energy balance schematic diagram is presented in Fig. 2.

The energy balance on each stage yields

$$\dot{Q}_i - h_{ii}A_{Ei}(T_{Bi} - T_{Ci}) = M_{Bi}C_p \frac{dT_{Bi}}{dt} + \dot{Q}_{lossi} \quad (1)$$

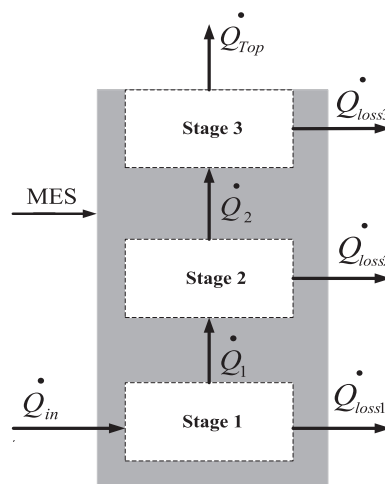


Fig. 2. Energy balance for the system.

Rearranging (1)

$$\dot{Q}_i - h_{ii}A_{Ei}(T_{Bi} - T_{Ci}) - \dot{Q}_{lossi} = M_{Bi}C_p \frac{dT_{Bi}}{dt} \quad (2)$$

$$h_{ii}A_{Si}(T_{Bi} - T_{Ci}) = h_{ii+1}A_{S1}(T_{Ci} - T_{Bi+1}) = \dot{Q}_1 \quad (3)$$

where “ h_{ii} ” (W/m²°C) is the internal heat transfer coefficient controlling heat transfer to $i + 1$ stage. “ T_{Bi} ” (°C) is the waterbed temperature in “ i th” stage ($i = 1, 2, 3$), “ T_{Ci} ” is the condensing surface temperature in “ i th” stage ($i = 1, 2, 3$), \dot{Q}_{lossi} (Watts) is the heat losses to ambient through insulation and fittings from “ i th” stage, “ A_{Ei} ” (m²) is the waterbed area in “ i th” stage, M_{Bi} (kg) is the mass of water in “ i th” stage, and “ \dot{Q}_i ” (Watts) is the heat input to “ i th” stage.

The heat input to the system is given by

$$\dot{Q}_{in} = \eta_c A_c I_b \quad (4)$$

where “ A_c ” is the area of collector (m²), “ I_b ” is the direct beam irradiation (W/m²), and “ η_c ” is the collection efficiency given by Eq. (5)

$$\eta_c = \frac{M_B C_p \Delta T + \dot{m}_{vi} L}{0.9 A_c I_b} \quad (5)$$

where “ \dot{Q}_{Top} ” (Watts) is the heat removed from top glass cover.

Mass balance for 1st, 2nd, and 3rd stage can be written as

$$\frac{dM_{Bi}}{dt} = -\dot{m}_{vi} \quad (6)$$

where “ \dot{m}_{vi} ” (kg/s) is the mass of distillate collected from i th stage.

Shatat and Mahkamov [5] used empirical equations for the determination of condensing surface temperature. According to their study, the surface temperature of condensing surface in a stage can be represented as a function of waterbed temperature in upper/next stage. For the last stage, the temperature of condensing surface can be expressed as a function of last stage’s waterbed temperature.

These equations can affect the accuracy in predicting the condensing surface’s temperature and hence, the distillate output due to their rigid nature. During the course of this work, it was found that the condensing surface temperature is a function of difference of

temperature between water bulk temperature of a particular stage and water bulk temperature of the next stage. The accuracy of model is improved when condensing surface temperature is expressed as a function of temperature difference. The empirical equations are given below:

For 1st stage,

$$\Delta T_{B12} = 0.98 - 0.96 T_{x1} + 0.21 T_{x1}^2 \quad (7)$$

$$T_{C1} = T_{B2} + \Delta T_{B12} \quad (8)$$

where

$$T_{x1} = T_{B1} - T_{B2} \quad (9)$$

2nd stage,

$$\Delta T_{B23} = 0.192 + 0.27 T_{x2} - 0.133 T_{x1}^2 \quad (10)$$

$$T_{C2} = T_{B3} + \Delta T_{B23} \quad (11)$$

where

$$T_{x2} = T_{B2} - T_{B3} \quad (12)$$

The temperature of condensing surface in 3rd stage is expressed as a function of waterbed temperature in that stage,

$$T_{C3} = T_{B3} + 1.1 \times 10^{-3} T_{B3}^3 - 0.135 T_{B3}^2 + 5.05 T_{B3} - 59.2 \quad (13)$$

2.4. Heat transfer coefficients

There are two kinds of heat transfer coefficients involved in MSS. The first one is internal heat transfer coefficient and the 2nd is external heat loss coefficient.

2.4.1. Internal heat transfer coefficient (h_{ii})

Within the stages of a MSS, heat transfer from bulk of water to covering/condensing surface is governed by convection, evaporation, and radiation. Collectively, these individual heat transfer coefficients are known as internal heat transfer coefficient.

$$h_{ii} = h_{CB} + h_{RB} + h_{EB} \quad (14)$$

2.4.2. Free convection (h_{CB})

The density variations in humid air as a result of temperature gradient in fluid cause heat transfer from waterbed to covering surface. The free convection coefficient in the upward direction through humid fluid is given by [9],

$$N_u = \frac{h_{CB}d_f}{K_f} = c(G_r P_r)^n \tag{15}$$

$$G_r = \frac{d_f^3 \rho_f^3 g \beta' \Delta T'}{\mu_f^2} \tag{16}$$

$$P_r = \frac{\mu_f C_f}{K_f} \tag{17}$$

$$\Delta T' = \left[(T_B - T_c) + \frac{(P_B - P_c)(T_B + 273)}{268.9 \times 10^3 - P_B} \right] \tag{18}$$

Different values of “ c ” and “ n ” based on “ G_r ” number range are available in literature. However, these values are sensitive to operating conditions and geometry of still. For a particular system, it is recommended to determine the values of “ c ” and “ n ” from experimental data. The method of determining these values has been discussed by Kumar and Tiwari [6] and details are given below.

Distillate output per hour is given as,

$$\dot{m}_v = 1.6273 \times 10^{-2} h_{CB} (P_B - P_C) \times \frac{3,600}{L} \tag{19}$$

rearranging (15),

$$h_{CB} = \frac{K_f c (G_r P_r)^n}{d_f} \tag{20}$$

substitution of (20) in (19) gives,

$$\frac{\dot{m}_v}{R} = c (G_r P_r)^n \tag{21}$$

where

$$R = 1.6273 \times 10^{-2} (P_B - P_C) \times \frac{3,600 K_f}{L d_f} \tag{22}$$

Eq. (21) is analogous to

$$y = ax^b$$

so that

$$y = \frac{\dot{m}_v}{R}; x = G_r \cdot P_r = Ra; a = c; \text{ and } b = n.$$

Finally, linear regression is performed to find the values of “ c ” and “ n ”. Once these values are established, the free convection coefficient can be determined using Eq. (15). The thermo-physical properties of humid air in solar still can be determined using equations given in Table 1.

2.4.3. Evaporative heat transfer coefficient (h_{EB})

Cooper [11] proposed the correlation for evaporative heat coefficient as a function of convective heat coefficient

$$h_{EB} = 1.6273 \times 10^{-2} h_{CB} \frac{(P_B - P_C)}{(T_B - T_C)} \tag{23}$$

Table 1
Thermo-physical properties of vapor-air mixture [10]

Property	Symbol	Equation
Specific heat capacity of fluid	C_f	$992.2 + 0.1434 T_{avg} + 1.01 \times 10^{-4} T_{avg}^2 - 6.758 \times 10^{-8} T_{avg}^3$
Density	ρ_f	$353.15 / (273.15 + T_{avg})$
Thermal conductivity	K_f	$0.0244 + 0.767310^{-4} T_{avg}$
Viscosity	μ_f	$1.71810^{-5} + 4.26 \times 10^{-8} T_{avg}$
Thermal expansion coefficient	β'	$1 / (273.15 + T_{avg})$
Latent heat of vaporization for water	L	$2.4935 \times 10^6 (1 - 9.4779 \times 10^{-4} T_{avg} + 1.3132 \times 10^{-7} T_{avg}^2 - 4.7974 \times 10^{-9} T_{avg}^3)$
Partial saturated vapor pressure at T_C	P_C	$\exp [25.3 - (5,144 / (273.15 + T_C))]$
Partial saturated vapor pressure at T_B	P_B	$\exp [25.3 - (5,144 / (273.15 + T_B))]$

2.4.4. Radiation heat coefficient (h_{RB})

For radiative heat coefficient, water surface and condensing surface are considered as infinite parallel planes. The radiation heat coefficient between infinite parallel planes is given by [9],

$$h_{RB} = \varepsilon_{EFF}\sigma[(T_B + 273)^2 + (T_C + 273)^2](T_B + T_C + 546) \quad (24)$$

where

$$\varepsilon_{EFF} = \left[\frac{1}{\varepsilon_{water}} + \frac{1}{\varepsilon_{GI}} - 1 \right]^{-1}$$

and “ σ ” is stefan-boltzmann constant ($5.67 \times 10^{-8} \text{ W/m}^2 \text{ K}^4$).

2.4.5. External loss coefficient

For the prediction of external heat losses from MSS the empirical relation discussed by Watmuf et al. [12] can be used. This expression for the external heat loss coefficient includes the effects of natural convection and radiation from MSS surface.

$$h_{EXT} = 5.7 + 3.8V \quad (25)$$

where “ V ” is the wind velocity in m/s.

2.5. Distilled water output

A simple heat balance for distillate can show that the mass flow rate of distillate produced is equal to the evaporation rate of saline water in each stage.

$$\dot{m}_{vi} = \frac{(T_{Bi} - T_{Ci})h_{EB}A_{Ei}}{L_i} \quad (26)$$

“ A_{Ei} ” (m^2) is the evaporation area in “ i th” stage.

These equations were used for writing the solar thermal desalination program in MATLAB. Further, additional information such as initial conditions and some other parameters were incorporated as input. These included:

- Initial water bulk temperature and height of water column in all stages.
- Dimensions of stages.
- Hourly average direct normal irradiation.
- Wind velocity.
- Average ambient temperature in day and weighted average temperature of night.

The developed model’s inputs and experimental conditions were synchronized in order to minimize variability in results. The experimental results were validated through the developed model. Once the model was validated with the experimental results, it was used for optimization and parametric studies of the process.

3. Results and discussion

The developed model for MSS system was used for the determination of still behavior during 24 h period. Required input data such as solar irradiation, ambient temperature, wind speed, and initial conditions of the day of experimentation were incorporated in the model. The model simulated the operation of MSS system for a 24 h period. The data from the model and experimentation were compared as shown in Figs. 3 and 4. The comparison of temperature profiles as predicted by model and the experimental results for 13 September 2012 is shown in Fig. 3.

To measure the variability in recorded measurements, standard error of the measurements was determined for the experimental test runs. Different test runs were performed at same operating temperature and nearly equal weather conditions. The maximum standard errors of measurement were found to be $\pm 0.03 \text{ kg}$, $\pm 0.02 \text{ kg}$, and $\pm 0.02 \text{ kg}$ for 1st, 2nd, and 3rd stage, respectively. The maximum error associated with hourly distillate yield of 1st stage can be explained by the distillate collection inaccuracies [13].

The cumulative distillate production from all the stages has been compared with experimental results in Fig. 4. The model showed a deviation of 6.8% in cumulative distillate production from 1st stage. The deviations in case of 2nd and 3rd stages distillate production were 14.2 and 6.6%, respectively. The model showed 6.4% deviation in overall cumulative distillate production. The maximum deviation for temperature prediction of 1st, 2nd, and 3rd stages were 7.7, 11.5, and 12.8%, respectively.

The comparison of model and experimental results for 22 December 2012 is shown in Figs. 5 and 6. Experimental cumulative product from individual stages and model predictions has been compared in Fig. 5, while the experimental and model temperature profiles are shown in Fig. 6. For this test run, the deviation in cumulative distillate for 1st, 2nd, and 3rd stages was determined to be 11.8, 9.5, and 7.3%, respectively. The overall distillate production showed 6.7% deviation. The maximum deviation in temperature prediction for every stage was determined to be 9.6, 10.9, and 14.9%, respectively.

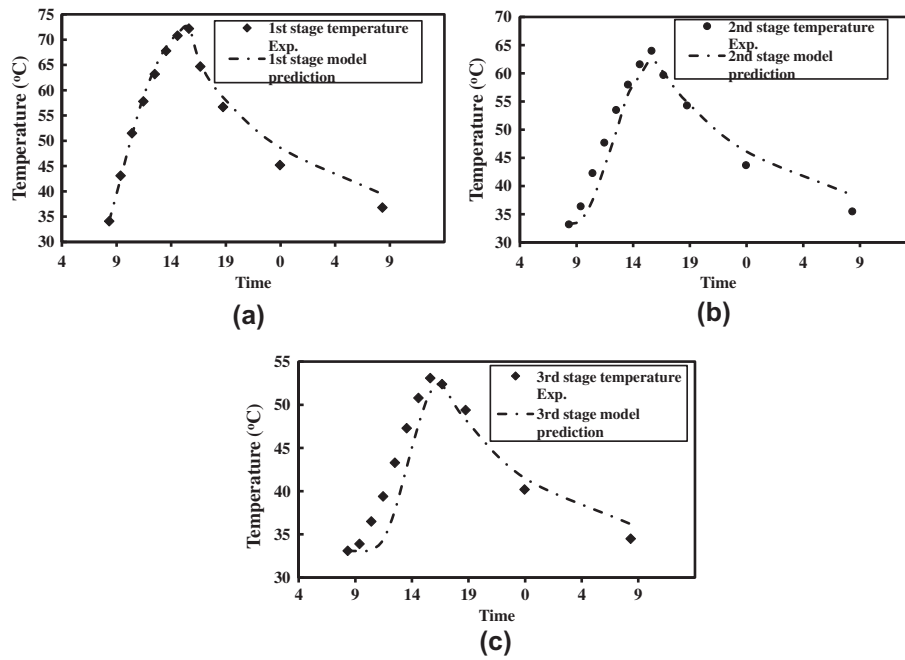


Fig. 3. Comparison of experimental and modeling results for stage temperatures (13 September 2012) (a) 1st stage; (b) 2nd stage; (c) 3rd stage.

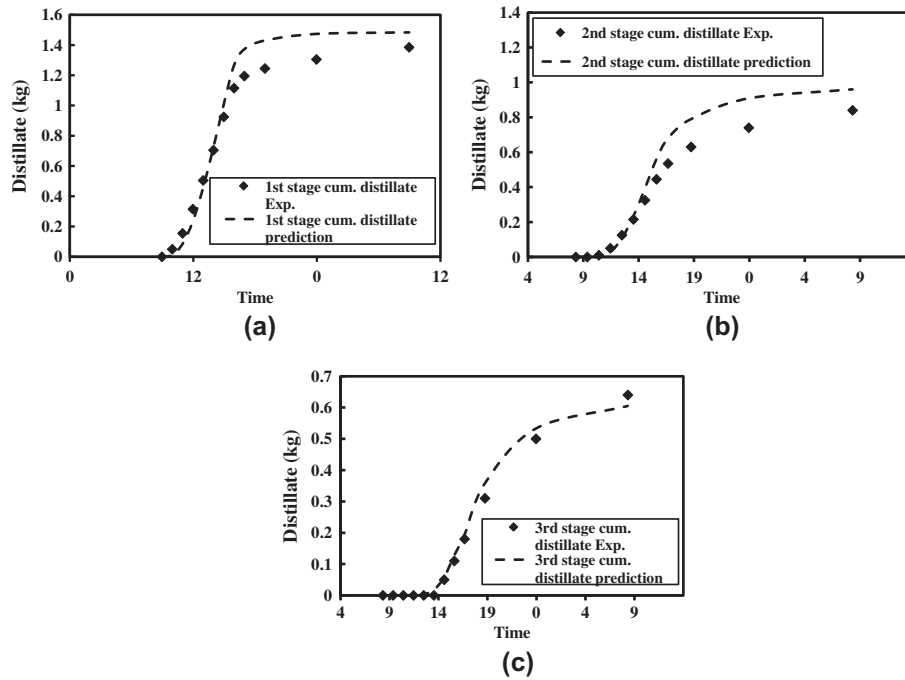


Fig. 4. Comparison of experimental and modeling results for distillate (13 September 2012) (a) 1st stage; (b) 2nd stage; (c) 3rd stage.

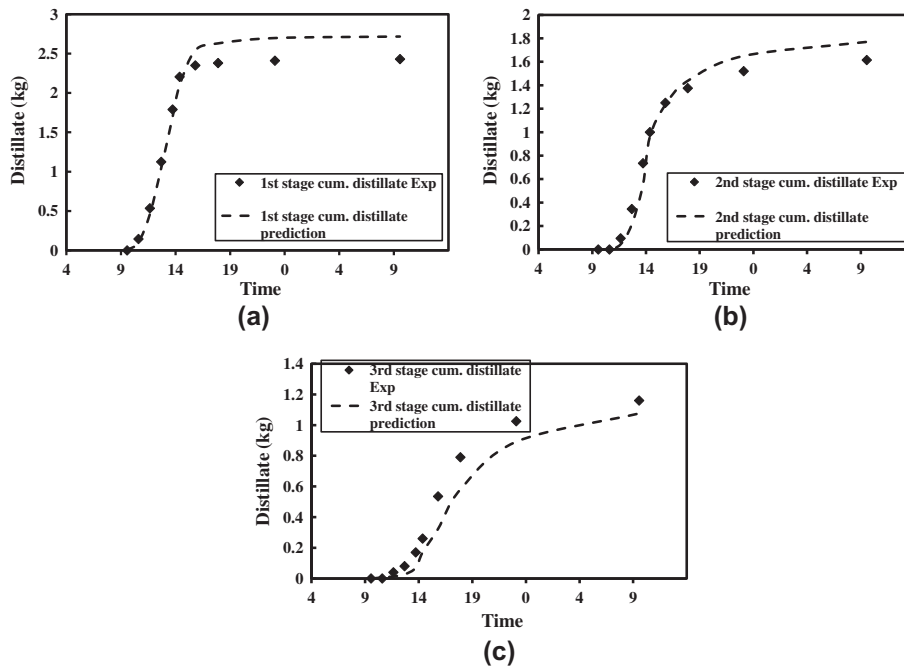


Fig. 5. Comparison of experimental and modeling results for distillate output (22 December 2012) (a) 1st stage; (b) 2nd stage; (c) 3rd stage.

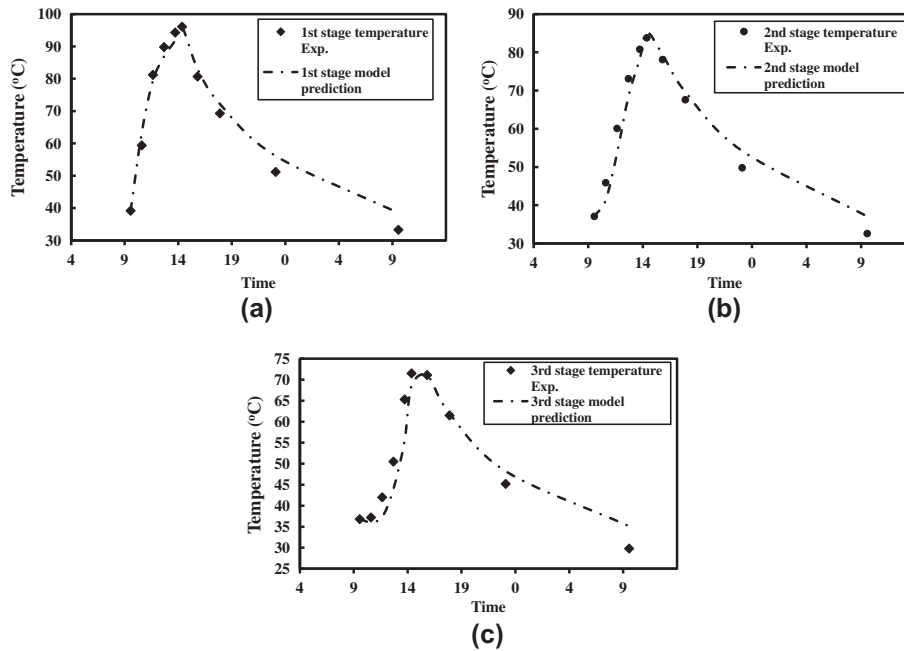


Fig. 6. Comparison of experimental and modeling results for stage temperatures (22 December 2012) (a) 1st stage; (b) 2nd stage; (c) 3rd.

Table 2
Summary of deviations for developed model

Test	1st stage distillate (%)	2nd stage distillate (%)	3rd stage distillate (%)	Overall product (%)
1	6.8	14.2	6.6	6.8
2	7.9	5.7	13.7	3.7
3	10.8	6.4	19.1	2.2
4	9.6	10.9	14.9	6.7
Average	8.8 ± 1.8	9.3 ± 4	13.6 ± 5.2	4.8 ± 2.3

Summary of deviation in distillate production from individual stages and overall distillate product has been presented in Table 2.

The average deviation in 1st stage output prediction was 8.8% with a standard deviation of 1.8%. However, for 2nd and 3rd stages, the average and standard deviation values were higher as compared to first stage. The 3rd stage distillate output could be disturbed due to abrupt changes in ambient conditions like low-wind speed during heating and high winds during cooling. The deviations in 3rd stage distillate output may affect the 2nd stage as well. The average deviation in overall distillate output of 4.8% with standard deviation of 2.3% showed good agreement with experimental results. The developed model served to determine the still performance in different seasons of year in next study.

The hourly average beam irradiation data for the year 2008 was used to determine the still productivity under different climates in a year. During the months of May and June the sun could be tracked for about 8 h (period during which the concentrated solar image can be focused on desired receiving area); due to high altitude of the sun in summers. Hence, the heating period increased up to 8 h. The total heat input in May was 23.5 MJ and the average hourly direct beam irradiation was 400–730 W/m². The maximum temperature for 1st, 2nd, and 3rd stage as predicted were 94,

89, and 74°C, respectively. The cumulative distillates from 1st, 2nd, and 3rd stages were 3.3, 2.3, and 1.6 kg, respectively. The still could produce a total distillate of 7.3 kg corresponds to 10 kg/m² d. The still productivity during different seasons has been summarized in Fig. 7.

The MSS specific daily production for the month of January, March, October, and December were 5.8, 7.8, 8.2, and 4.8 kg/m² d, respectively. The MSS productivity varied due to direct beam irradiation and the sun tracking time. Islam et al. [14] measured the direct beam irradiation at Abu Dhabi for the year 2007. According to this study, the direct beam irradiation was higher in the months of transition periods (summer to winter and vice versa).

During the month of March, the system produced 7.8 kg/m² d for a heat input of 23.3 MJ and sun tracking time of 6 h. In December, the system produced 4.8 kg/m² d for a heat input of 15.9 MJ for 5 h of sun tracking. Direct beam irradiation for all the months remained more than 400 W/m². This value was best suited for concentrated type solar collectors.

The developed model could determine optimum design parameter for maximum still output. The effect of varying stage spacing known as characteristic length (distance between water surface and condensing surface) was studied by Ahmed et al. [4]. According to their study, the optimum spacing was 25 cm. However, no information was reported for spacing lower than 25 cm. The designed stage spacing for the MSS system was 20 cm. The height of distillate collection trough including the distance between waterbed and collection trough was almost 70 mm. Therefore, design constraint of 100 mm was set to be the lower bound on stage spacing. The developed model was used for the determination of still productivity, when the stage spacing was 10, 15, 20, 25, and 30. The modeling results are shown in Fig. 8.

The optimum spacing determined to be 10 cm having specific production capacity of 10.6 kg/m² d. The production capacity decreased sharply with increase in stage spacing and remained constant for higher stage spacing.

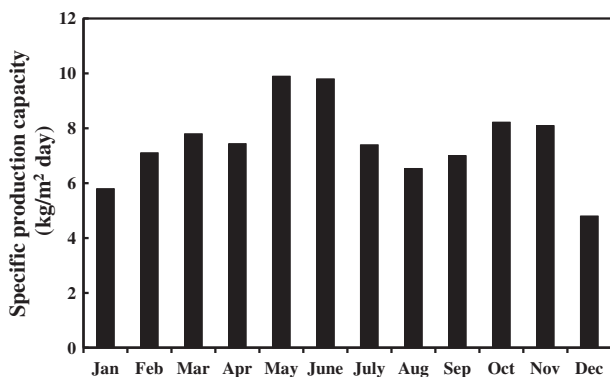


Fig. 7. Seasonal productivity.

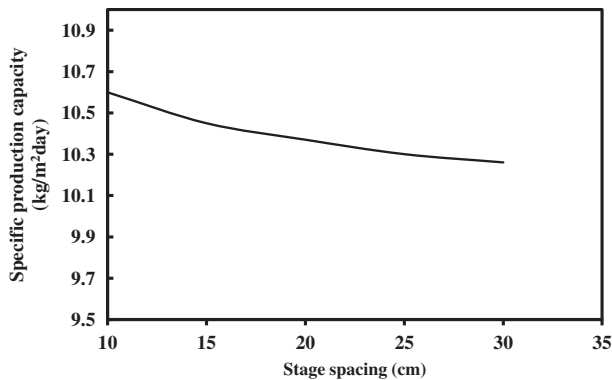


Fig. 8. Effect of stage spacing on MSS productivity.

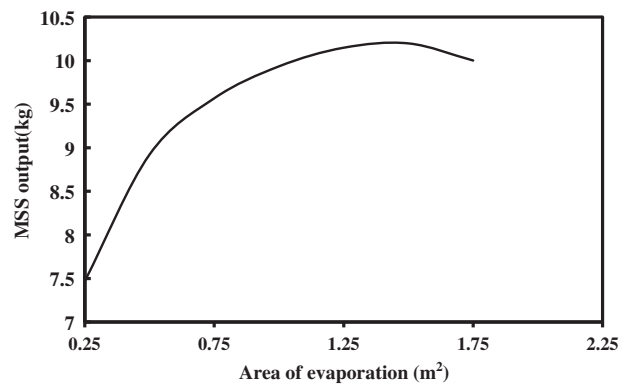


Fig. 10. Effect of evaporation area on still output.

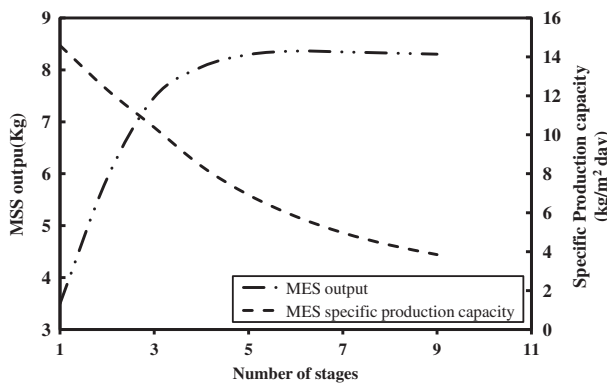


Fig. 9. Effect of number of stages on MSS output and productivity.

The effect of number of stages on MSS output and specific production capacity is shown in Fig. 9. Simulations were performed for stages ranging from 1 to 9. It was evident that the MSS output increased up to five stages. The addition of further stages seemed to have no significant improvement in the output of MSS. The maximum MSS output for five stages was determined to be 8.3 kg. Lower output of MSS with the additional stages was due to lower vapor production from successive stages. The specific production capacity decreased due to increase in added total evaporation area.

Generally, as evaporation area increases, the rate of evaporation also increases. The effect of evaporation area in every individual stage was studied by changing the evaporation area in each stage. Evaporation area was simulated from 0.25 to 1.75 m² with 0.25 m² increment and the results are shown in Fig. 10. The maximum MSS output reached 10 kg at 1.5 m² and then decreased gradually at 1.75 m². As evaporation area increases, total surface area increases, subsequently heat losses increases and MSS output will be less.

Maximum daily yield with output optimized parameters was predicted to be 13.5 kg. The operating temperatures were predicted to be in the range of 50–80°C. This indicated that the Fresnel lens (area 1.373 m²) was not providing required energy to the system. Further simulations were performed with optimized parameters and different lens areas. A lens area of 2.2 m² with daily yield of 25 kg was obtained at operating temperature ranges from 60 to 95°C.

It was noted that adding more stages yield higher still output. However, the increase in output with the addition of a new stage is lower than the increase in output with previously added stage. Similarly, higher evaporation area results in higher still output up to a certain range. Moreover, adding more number of stages will result additional cost for the construction of MSS. Thus, requirement of capital expenditures will be more. Therefore, a balance between capital expenditure and benefit should be carried out to determine the optimized parameters.

The study of Adhikari and Kumar [15] provided a guide for the cost optimization of MSS parameters. The simulations for a particular number of stages and different feasible evaporation areas (denoted as “R”; ratio of collector area to still base) were performed for a complete year. The annual production capacity and the various costs for MSS were used for the determination of unit production cost. Thus, production cost served as a measure for the determination of cost-optimized parameters.

The upper and lower bound of feasible number of stages and evaporation area were determined from output optimization analysis. For a collector area of 2.2 m², different values of “R” used were 2.9, 2.2, 1.76, and 1.46 corresponds to stage evaporation area of 0.75, 1, 1.25, and 1.5 m², respectively. The annual production as a function of number of stages and evaporation area is shown in Fig. 11. The slope of each

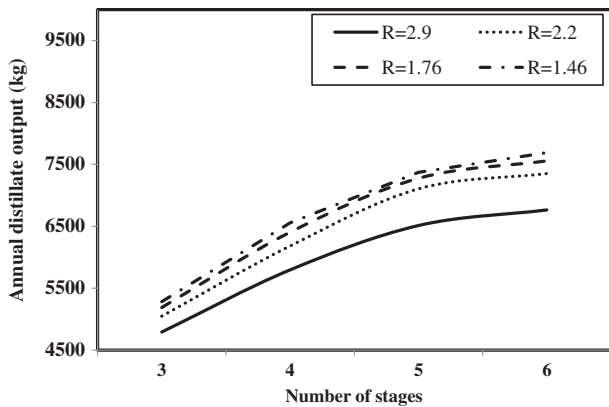


Fig. 11. Annual output as a function of number of stages, evaporation area, and collector area.

individual line showed the effect of adding number of stages on annual output of MSS system.

The distance between each line represented the effect of added evaporation area on annual output of MSS system. This trend clearly indicated the requirement of cost analysis. The annual cost of total system is given by Eq. (27) [15].

$$C_T = C_{sf_s} + C_{cf_c} + C_{track}f_{track} + M_s C_s + M_c C_c + M_{track} C_{track} - (S_s F_s C_s + S_c F_c C_c + S_{track} F_{track} C_{track}) \quad (27)$$

where C_s , C_c , and C_{track} are the capital expenditure for MSS, Fresnel lens and auto tracking system, respectively. M_s , M_c , and M_{track} are the annual maintenance cost for MSS, Fresnel lens, and tracking system, respectively. The salvage value of MSS, Fresnel lens, and auto tracking system are given by S_s , S_c , and S_{track} respectively. The capital recovery factor for MSS, Fresnel lens and auto tracking system are f_s , f_c , and f_{track} . F_s , F_c , and F_{track} are the sinking fund factors for MSS, Fresnel lens, and auto tracking system, respectively. The capital recovery factor and sinking fund factors are given by Eqs. (28) and (29).

$$f = \frac{i(1+i)^n}{(1+i)^n - 1} \quad (28)$$

$$F = \frac{i}{(1+i)^n - 1} \quad (29)$$

where “ i ” is the interest rate and “ n ” is the lifespan of project. Different costs associated with MSS system are shown in Table 3.

Table 3
Costs of components involved in MSS system

Material cost	Value
Galvanized Iron sheets (2 mm) (local market)	\$ 0.9/kg
Copper plate (2 mm) (local market)	\$ 9/kg
Thermocol insulation (50 mm) (local)	\$ 2/m ²
Others (glass sheets, sealant etc.)	3% (GI and insulation)
Fresnel lens (China)	\$120/m ²
Auto-tracking system	25% (cap-ex)
Cost of labor	15% (GI and insulation)
Overhead cost	20% (GI and insulation)
Maintenance cost	
MSS (paint and cleaning)	3% (cost for MSS)
Fresnel lens	3% (cost for Fresnel lens)
Auto tracker	5% (cost for auto tracker)
Salvage value	
MSS	10% (cost of MSS)
Fresnel lens	10% (cost of Fresnel lens)
Auto tracker	15% (cost of auto tracker)
Net rate of interest discounting for rate of inflation	0.12

The unit production cost for MSS system is given by Eq. (30).

$$C_p = \frac{C_T}{M_y} \quad (30)$$

where “ M_y ” is the annual production cost.

For an operating lifespan of five years (based on “GI”), the unit production cost is shown in Fig. 12 for different number of stages with varying “ R ”.

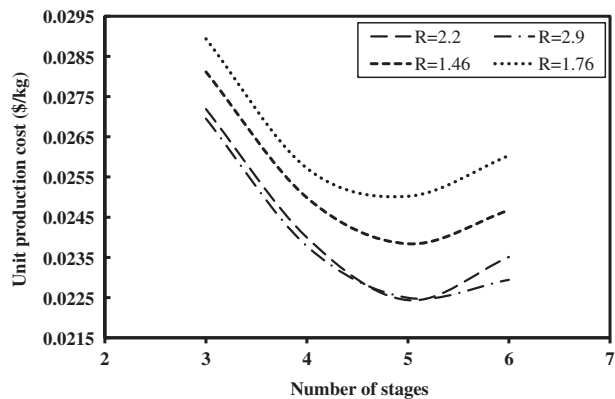


Fig. 12. Unit production cost as function of number of stages, evaporation area, and collector area.

Table 4
Comparison of different parameters for various desalination units

Ref.	Type of system	Area of evaporation (m ²)	Area of collector (m ²)	Productivity (evaporation area) (kg/m ² d)	Productivity (Collector area) (kg/m ² d)	Plant capacity (kg/d)
[16]	Passive solar still	0.54	0.54	3.12	3.12	1.65
[5]	MSS-ETC	5	2.2	4.3	9.7	21.5
[4]	MSS	–	–	–	9	–
[17]	MSS	–	7.8	–	9.4	73.6
[3]	2 effect-CPC	2	2	7.3	7.3	14.7
Current study	MSS-Fresnel lens	5	2.2	4.8	10.9	24

The optimum number of stages and evaporation area based on optimum unit production cost were determined to be 5 and 1 m², respectively. The production cost corresponds to these parameters was determined to be \$ 0.02234/kg (AED 0.083/kg) or \$ 22.34/m². With these optimized parameters, the still produce a maximum output of 24 kg corresponds to a specific production capacity of 4.8 kg/m² d (based on evaporation area) and 10.9 kg/m² d (based on collector area). The payback period for the system is 11 months based on bottled water price in UAE (\$ 0.086/L). The current MSS system has been briefly compared with previously developed systems in Table 4.

Some of the previous researchers reported unit production cost in the range of \$15–25/m³ for the systems described in Table 4. The developed MSS system in this research work is quite satisfactory in comparison to previously developed systems having unit production cost below \$ 0.025/kg. The production cost can be lowered further using nickel-aluminum bronze which is best suited for seawater applications (low corrosion rate) which increases lifespan up to 10–15 years.

4. Conclusion

The developed mathematical model showed 8.8, 9.3, and 13.6% average deviation in distillate prediction from 1st, 2nd, and 3rd stages, respectively. Seasonal variations predicted by the model showed that the system can achieve a maximum specific production capacity of 10 kg/m² d in the month of May, which showed almost threefold improvement of output when compared to a single-basin solar still. The optimization of systems' physical dimension to enhance the MSS output suggests that the stage spacing that will result in maximum output was found to be 10 cm through simulations conducted with

different feasible stage spacing. The optimum number of stages that will maximize the MSS output was determined to be 5. However, cost analysis is required to decide the number of stages. The increase in evaporation area increased the output of MSS up to 1.25 m². The added evaporation area increased the cost of MSS and requires a cost analysis before deciding any values. The maximum output of MSS based on cost optimized parameters was determined to be 24 kg. The present system will be the best choice for scenarios involving small foot print area, low skilled labor, low maintenance cost, and high distillate quality.

Acknowledgment

The authors are thankful to Dr Priyabrata Pal for his kind help.

Nomenclature

A_C	— area of condensing surface (m ²)
A_E	— area of evaporation surface (m ²)
C_p	— heat capacity of water (J/kg°C)
C_f	— heat capacity of vapor air mixture (J/kg°C)
c	— constant
d_f	— characteristic length distance between waterbed surface and condensing surface (m)
G_r	— Grashof number
h_{CB}	— convective heat coefficient (W/m ² K)
h_{EB}	— evaporative heat coefficient (W/m ² K)
h_{RB}	— radiation heat coefficient (W/m ² K)
h_{ii}	— overall internal heat coefficient (W/m ² K)
h_{EXT}	— overall external heat coefficient (W/m ² K)
I_b	— direct beam irradiation (W/m ²)
K	— thermal conductivity of moist air (W/m K)
L	— latent heat of vaporization (J/kg K)
\dot{m}_{vi}	— Distillate rate (kg/s)
M_B	— mass of waterbed (kg)
n	— constant

N_{iu}	— Nusselt number
P_B	— partial saturated vapor pressure near bed surface (K Pa)
P_C	— partial saturated vapor pressure at condensing surface (K Pa)
P_r	— Prandtl number
\dot{Q}_{in}	— heat input to 1st stage (J/s)
\dot{Q}_2	— heat input to 2nd stage (J/s)
\dot{Q}_3	— heat input to 3rd stage (J/s)
\dot{Q}_{lossi}	— heat losses from sides (J/s)
\dot{Q}_{Top}	— heat losses from top cover (J/s)
T_{Bi}	— temperature of waterbed in i th stage ($^{\circ}\text{C}$)
T_{Ci}	— temperature of condensing surface in i th stage ($^{\circ}\text{C}$)
T_{avg}	— average temperature of T_B and T_C
t	— time
V	— wind velocity (m/s)

Greek symbols

β'	— thermal expansion coefficient (K $^{-1}$)
ρ_f	— density of humid fluid (kg/m 3)
μ_f	— viscosity of humid fluid (kg/m sec)
σ	— Stefan Boltzmann constant (5.67×10^{-8} W/m 2 K 4)
ε	— emissivity of material

Subscript

i	— stage number ($i = 1, 2, 3$)
GI	— Galvanized iron

References

- [1] G.N. Tiwari, S.A. Lawrence, S.P. Gupta, Analytical study of multi-effect solar still, *Energy Convers. Manage.* 29(4) (1989) 259–263.
- [2] R.S. Adhikari, A. Kumar, Transient simulation studies on a multi-stage stacked tray solar still, *Desalination* 91(1) (1993) 1–20.
- [3] B. Prasad, G.N. Tiwari, Analysis of double effect active solar distillation, *Energy Convers. Manage.* 37(11) (1996) 1647–1656.
- [4] M.I. Ahmed, M. Hrairi, A.F. Ismail, On the characteristics of multistage evacuated solar distillation, *Renewable Energy* 34(6) (2009) 1471–1478.
- [5] M.I.M. Shatat, K. Mahkamov, Determination of rational design parameters of a multi-stage solar water desalination still using transient mathematical modeling, *Renewable Energy* 35(1) (2010) 52–61.
- [6] S. Kumar, G.N. Tiwari, Estimation of convective mass transfer in solar distillation systems, *Sol. Energy* 57(6) (1996) 459–464.
- [7] S. Aggarwal, G.N. Tiwari, Convective mass transfer in a double-condensing chamber and a conventional solar still, *Desalination* 115(2) (1998) 181–188.
- [8] H. Khaoula, B. Ali, B.S. Rhomdanne, G. Slimane, Effects of SSD and SSDHP on convective heat transfer coefficient and yields, *Desalination* 249(3) (2009) 1259–1264.
- [9] G.N. Tiwari, *Solar Energy: Fundamentals, Design, Modeling and Applications*, CRC Press, New Delhi, 2002.
- [10] D. Jain, G.N. Tiwari, Thermal aspects of open sun drying of various crops, *Energy* 28(1) (2003) 37–54.
- [11] P.I. Cooper, The maximum efficiency of single-effect solar stills, *Sol. Energy* 15(3) (1973) 205–217.
- [12] J. Watmuf, W. Charters, D. Proctor, Solar and wind induced external coefficients—Solar collectors, *Cooperation Mediterranee pour l'Energie Solaire, Revue Internationale d'Heliotechnique* 2nd quarter (1977) 56.
- [13] O. Younas, F. Banat, D. Islam, Performance assessment of a multi-stage solar still coupled with fresnel lens for water desalination, *Therm. Energy Power Eng.* 2(4) (2013) 164–170.
- [14] M.D. Islam, A.A. Alili, I. Kubo, M. Ohadi, Measurement of solar-energy (direct beam radiation) in Abu Dhabi, UAE, *Renewable Energy* 35(2) (2010) 515–519.
- [15] R.S. Adhikari, A. Kumar, Cost optimization studies on a multi-stage stacked tray solar still, *Desalination* 125 (1–3) (1999) 115–121.
- [16] A.E. Kabeel, A.M. Hamed, S.A. El-Agouz, Cost analysis of different solar still configurations, *Energy* 35(7) (2010) 2901–2908.
- [17] H. Nishikawa, T. Tsuchiya, Y. Narasaki, I. Kamiya, H. Sato, Triple effect evacuated solar still system for getting fresh water from seawater, *Appl. Therm. Eng.* 18(11) (1998) 1067–1075.